

Electron Density Profile Behavior during SMBI Measured with AM Reflectometer in Heliotron J Plasma

Kiyofumi MUKAI, Kazunobu NAGASAKI¹⁾, Tohru MIZUUCHI¹⁾, Vladimir ZHURAVLEV²⁾, Shinsuke OHSHIMA³⁾, Takeshi FUKUDA⁴⁾, Takashi MINAMI¹⁾, Hiroyuki OKADA¹⁾, Shinji KOBAYASHI¹⁾, Satoshi YAMAMOTO¹⁾, Yuji NAKAMURA, Kiyoshi HANATANI¹⁾, Shigeru KONOSHIMA¹⁾, Masaki TAKEUCHI¹⁾, Koji MIZUNO, Hyunyong LEE and Fumimichi SANO¹⁾

Graduate School of Energy Science, Kyoto University, Gokasho, Uji 611-0011, Japan

¹⁾ *Institute of Advanced Energy, Kyoto University, Gokasho, Uji 611-0011, Japan*

²⁾ *RRC “Kurchatov Institute”, Institute of Nuclear Fusion, Moscow 123182, Russia*

³⁾ *Pioneering Research Unit for Next Generation, Kyoto University, Gokasho, Uji 611-0011, Japan*

⁴⁾ *Center for Atomic and Molecular Technologies, Osaka University, 2-1 Yamadaoka, Suita 565-0871, Japan*

(Received 19 March 2011 / Accepted 31 May 2011)

The electron density profile was measured using a microwave amplitude modulation (AM) reflectometer in Heliotron J plasmas, where plasma performance was improved using supersonic molecular beam injection (SMBI) as a fueling method. Immediately after the SMBI pulse, for the case in which the supersonic molecular beam penetrates deeply, the density profile rapidly peaks, and the electron density increases in both core and edge regions. Afterward, while the line-averaged electron density is monotonically increasing, the density profile becomes more peaked. In this phase, the edge electron density measured by a Langmuir probe decreases and the peaking factor of the SX profiles measured by an absolute extreme ultraviolet array increases. These trends are consistent with the electron density trend determined by the AM reflectometer. SMBI affects particle confinement and transport, thus possibly increasing plasma stored energy.

© 2011 The Japan Society of Plasma Science and Nuclear Fusion Research

Keywords: density profile, reflectometer, SMBI, fueling control, particle confinement, Heliotron J

DOI: 10.1585/pfr.6.1402111

1. Introduction

Fueling control is one of the most important issues in magnetically confined plasma research, because it is necessary to achieve high-density and high-performance plasmas. Compared with the conventional gas puffing method, the supersonic molecular beam injection (SMBI) method [1] is efficient in obtaining deeper penetration of neutral particles into the core plasma. An SMBI system has been applied to Heliotron J since 2008, and we successfully extended the operation region of line-averaged electron density (\bar{n}_e) versus plasma stored energy (W_p) by using this method [2]. Measurement of the plasma profile is required to investigate how SMBI improves plasma confinement. An amplitude modulation (AM) reflectometer is useful for measuring the electron density profile. AM reflectometer is a technique to detect the envelope phase of the amplitude-modulated microwave in order to reduce the effect of density fluctuations and fringe jumps in the profile measurement [3]. This system has been applied to measure the electron density profiles in T-10 tokamak [4], W7-AS [5], TJ-II [6] and HL-2A [7], and to study particle confinement improvement [8, 9]. We recently installed an

AM reflectometer for Heliotron J and start to measure the electron density profiles [10].

This paper describes the experimental results of the electron density profile measurement in Heliotron J SMBI plasmas by using the AM reflectometer. The remainder of this paper is organized as follows. In Sec. 2, the experimental set-ups of Heliotron J, its gas fueling system and its AM reflectometer are described. In Sec. 3, the behavior of the electron density profiles is described both during and after SMBI, and the results are summarized in Sec. 4.

2. Experimental Set-up

2.1 Heliotron J

Heliotron J is a medium-sized helical-axis heliotron device ($\langle R_0 \rangle = 1.2$ m, $\langle a \rangle = 0.17$ m and $\langle B_0 \rangle \leq 1.5$ T) with a helical coil ($L/M = 1/4$) [11]. The locations of the heating, diagnostic, and gas-fueling systems are shown in Fig. 1. The initial plasmas are produced using a second-harmonic X-mode ECH (70 GHz, 0.4 MW) at the port #9.5. In this experiment, additional heating is performed by using two tangential NBI systems of hydrogen beams (30 kV, 0.7 MW). BL-1 (#2.5) and BL-2 (#6.5) are counter and co-injection, respectively, under this experimental con-

author's e-mail: mukai@center.iae.kyoto-u.ac.jp

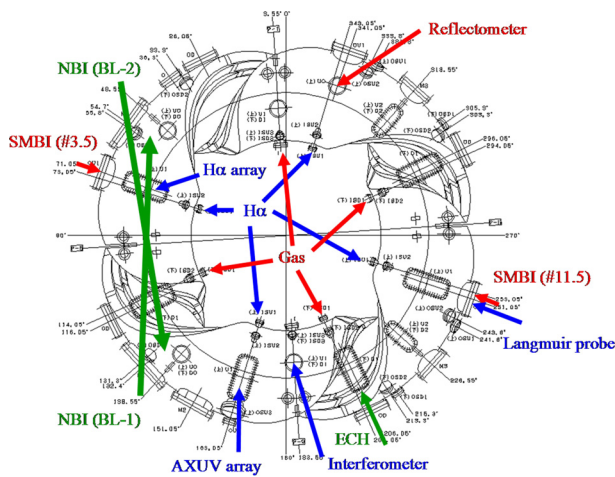


Fig. 1 Locations of the heating, diagnostic, and gas fueling systems in Heliotron J.

dition of normal magnetic field direction.

The electron density profile is measured using an AM reflectometer at #15.5 port, as described in detail in Sec.2.3. A 130 GHz interferometer is installed at #8.5 for \bar{n}_e measurement. The edge density is measured with a movable Langmuir probe at #11.5. An H α array system at #3.5 is used to estimate the deposition position of the supersonic molecular beam (SMB). An absolute extreme ultraviolet (AXUV) array with an Al 1 μ m filter is used to observe the SX profile (> 100 eV mainly) at #7.5.

2.2 Gas-fueling system

Two SMBI systems with hydrogen are installed at #3.5 and #11.5 ports. In this experiment, the SMBI #3.5 is used. It consists of a fast piezoelectric valve with a short conic-nozzle with 0.2 mm ϕ . The speed of the SMB is estimated to be 1.3-1.6 km/s for a plenum pressure of 1.0-1.5 MPa by using the “time of flight” method [12].

Density is usually controlled using a gas puffing system with piezoelectric valves. The amount of gas injected is controlled by applying voltage to the valves of #5.5, #9.5, #13.5 and #16.5 (deuterium), #5.5 and #9.5 (hydrogen) ports.

2.3 AM reflectometer

A microwave AM reflectometer for the electron density profile measurement was installed in the 2009 experimental campaign [10]. The schematic representation of the reflectometer is shown in Fig. 2. An AM-type system is adopted to reduce the density fluctuation effects during the profile measurement. The X-mode is selected as the propagation mode to measure the flat or hollow density profile that is typically observed in the ECH plasmas of helical devices. In fact, the flat or hollow profiles have been measured in Heliotron J ECH plasmas [10]. The carrier frequency of the reflectometer ranges from 33 to 56 GHz, and

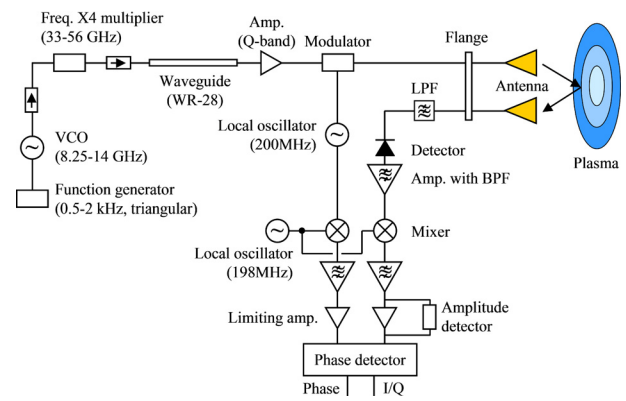


Fig. 2 Schematic representation of AM reflectometer.

can be swept linearly with a sweeping frequency of up to 2 kHz for the electron density profile measurement. The modulation frequency is 200 MHz.

In this system, two assumptions are made to reconstruct the electron density profile: (1) one is that the electron density at $\rho = 1.2$ is zero and (2) the other is that the density linearly increases between $\rho = 1.2$ and the most outside point that can be measured with this system.

3. Electron Density Profile Behavior in SMBI Plasma

3.1 Electron density profile behavior during SMBI

To study the time evolution of the electron density profile, comparison between directional and non-directional SMBI was carried out under the same heating condition by using a movable shutter placed in front of the SMBI #3.5. When the shutter is closed, the ejected SMB from the nozzle is blocked by the shutter and injected into the plasma in a manner similar to that of gas puffing. Figures 3 (a) and (b) shows the time evolution of \bar{n}_e , W_p , and H α for ECH + NBI plasmas for the cases of an open and a closed shutter,

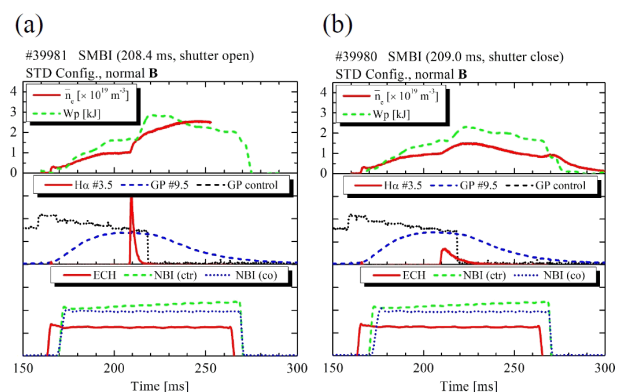


Fig. 3 Time evolution of \bar{n}_e , W_p and H α for ECH+NBI plasmas for (a) an open shutter and (b) a closed shutter.

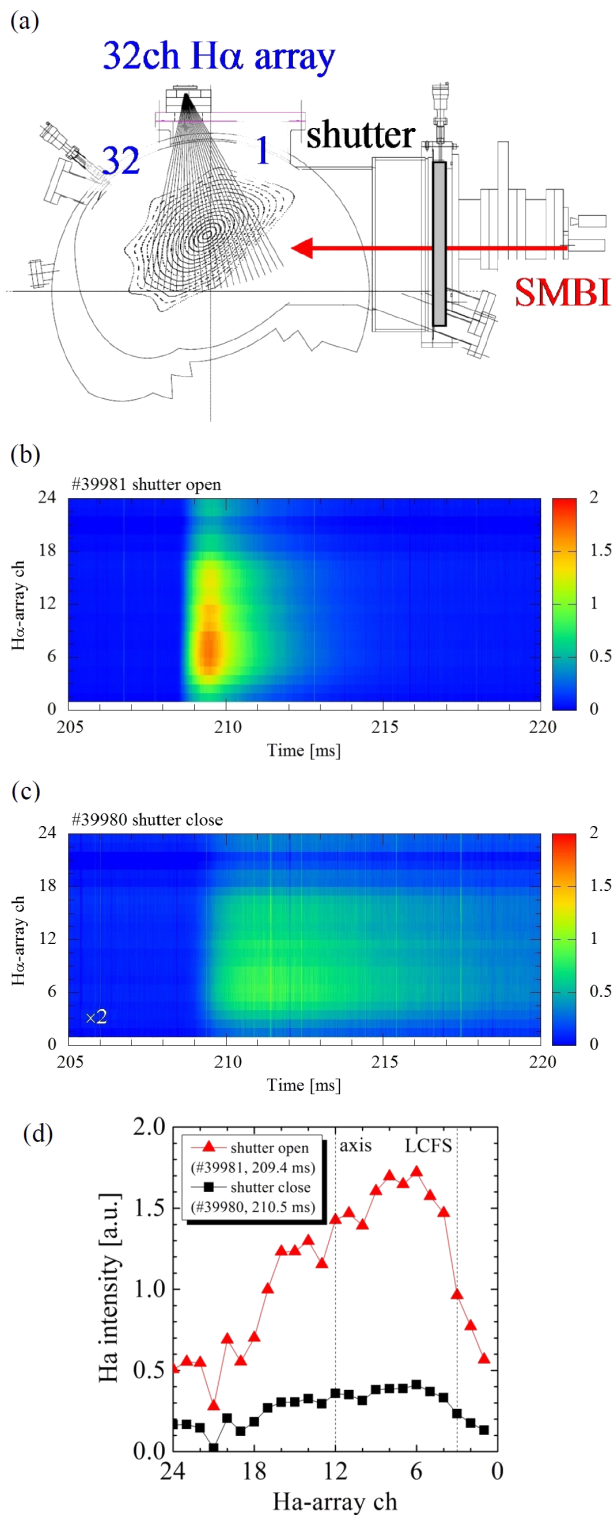


Fig. 4 Sight line of H α array (a), time evolution of H α array for the case of (b) open shutter and (c) closed shutter ($\times 2$), and radial profiles for these two cases (d).

respectively. SMBI increases H α #3.5 in SMBI pulse timing, and the injection time of SMB is determined as the rise time of H α #3.5. The sight line of the H α array is shown in Fig. 4 (a), and the time evolution of the H α array is shown in Figs. 4 (b) and (c). Ch 3 and ch 12 correspond to the

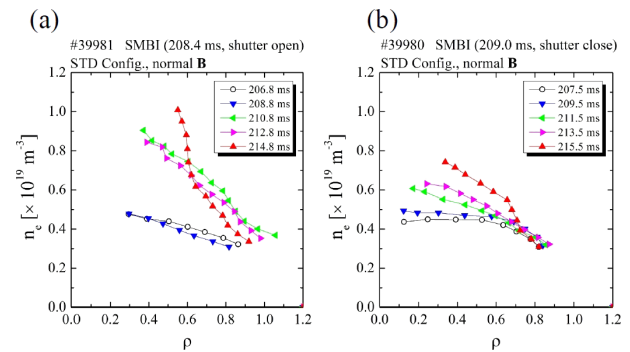


Fig. 5 Time evolution of n_e profile for the cases of (a) open shutter and (b) closed shutter.

LCFS and magnetic axis, respectively. The radial profiles at around 210 ms are shown in Fig. 4 (d). In the open shutter case, the SMB penetrates toward the magnetic axis and deposits more, and the H α intensity outside the torus is obviously higher than that inside the torus. However, to estimate the penetration length of the neutral particles, it is necessary to measure from one more direction. Figure 5 shows the time evolution of the density profile measured with the AM reflectometer for the cases of an open and a closed shutter. Each profile is reconstructed from the data time averaged over 2 ms. In the open shutter case, the electron density increases rapidly in the core region and the density profile changes rapidly to a peaked one; however, in the closed shutter case, density profile change is modest.

3.2 Electron density profile behavior after SMBI

The SMBI and conventional gas puffing methods were compared to study the change in the density profile after SMBI. Figures 6 (a)-(c) and (d)-(f) shows the time evolution of \bar{n}_e , W_p , and H α for NBI only heating plasmas for the cases of the SMBI and conventional gas puffing methods, respectively. The SMB is injected for 216.4 ms. After the SMBI pulse, \bar{n}_e continues to increase, while W_p decreases rapidly for ~ 6 ms and then starts to increase. The dependence of W_p on \bar{n}_e is shown in Fig. 7. Compared with the plasma using conventional gas puffing, higher maximum values of \bar{n}_e and W_p were obtained in that using SMBI. These results indicate that SMBI improves plasma confinement at $\bar{n}_e > 3.5 \times 10^{19} \text{ m}^{-3}$ better than conventional gas puffing.

The time evolution of the density profile under the two fueling systems is shown in Fig. 8. Each profile is reconstructed from the time averaged data obtained over 2 ms in the same manner as that in Sec. 3.1. In the SMBI plasma, immediately after the SMBI pulse at 218.3 ms, the electron density increases in both the core and edge regions as described in Sec. 3.1. Next, however, the density near $\rho \sim 0.6$ decreases to a minimum at 232.3 ms and then increases again at 238.3 ms, while \bar{n}_e continues to increase.

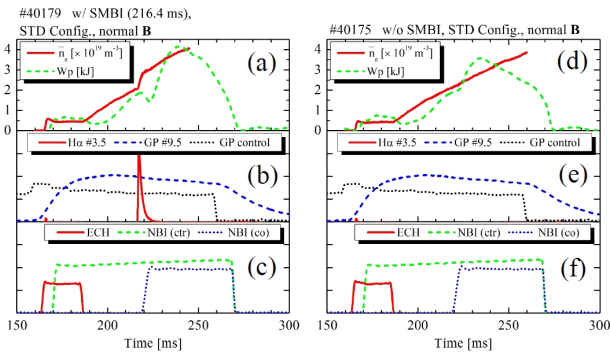


Fig. 6 Time evolution of \bar{n}_e , W_p and $H\alpha$ for NBI only heating plasmas in the case of (a)-(c) SMBI and (d)-(f) conventional gas puffing.

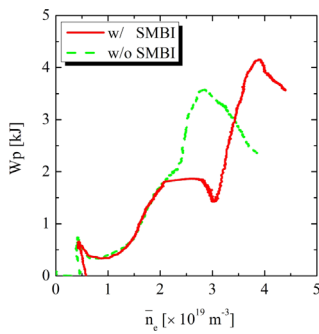


Fig. 7 Dependence of W_p on \bar{n}_e for the cases of SMBI and conventional gas puffing.

These results imply that density peaking in the core region of plasma considerably increases around 232.3 ms. In this phase, W_p increases rapidly. In contrast, in conventional gas puffing, density profile change is modest, as shown in Fig. 8 (b). SMBI affects particle confinement and transport, thus possibly increasing W_p .

Figure 9 shows the time evolution of the density profile, edge density, phase signal of the reflectometer, peaking factor of the AXUV profile, and \bar{n}_e and W_p under the (a)-(e) SMBI and (f)-(h) conventional gas puffing conditions. The edge density at $\rho = 0.9$ is plotted in Fig. 9 (b). Another edge density is measured with a movable Langmuir probe at #11.5. In this discharge, the measurement position is 5 mm outside the LCFS. The edge density rapidly increases immediately after the SMBI pulse and then decreases from 218.6 to 233.3 ms. The reflectometer and Langmuir probe measurements show similar trends although the S/N ratio is not sufficiently high in the profile measurement. In contrast, the phase signal changes with the local density more accurately when the carrier frequency is fixed. The phase data shown in Fig. 9 (c) are measured at the fixed carrier frequency of 48 GHz which corresponds to the cutoff position of $\rho \sim 0.6$. Note that the data are measured during another discharge but under the same condition. When the local density at the mea-

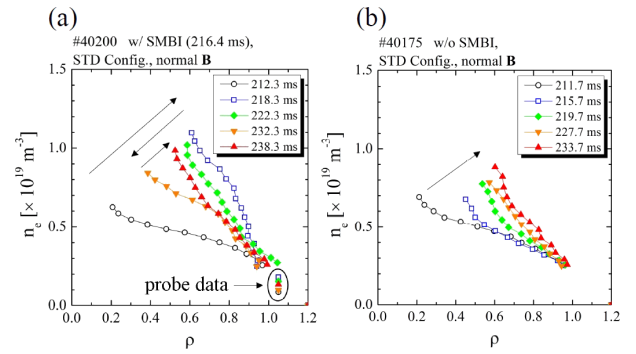


Fig. 8 Time evolution of n_e profile for the cases of (a) SMBI and (b) conventional gas puffing.

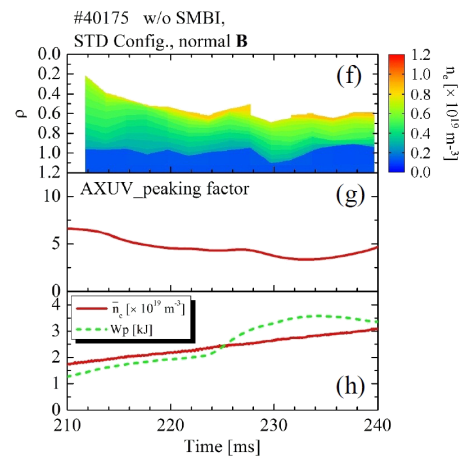
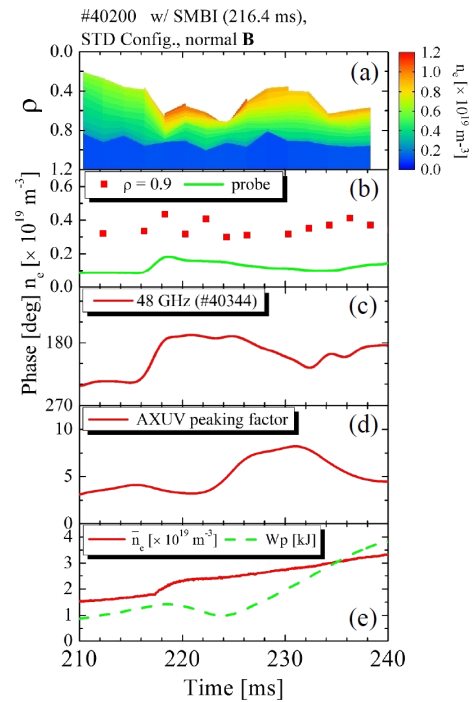


Fig. 9 Time evolution of n_e profile, edge density, phase signal of reflectometer, peaking factor of AXUV profile, \bar{n}_e , and W_p for (a)-(e) SMBI and (f)-(h) conventional gas puffing.

surement position increases, the position of the cutoff layer moves outward and the phase signal decreases. The density around $\rho \sim 0.6$ also rapidly increase just after SMBI pulse and reaches the minimum values at 232.4 ms. The peaking factor of the AXUV array is calculated from the ratio of the sight line of the magnetic axis and $\rho = 0.6$. The peaking factor of the AXUV profile reaches its maximum at 231.2 ms. These results suggest that the density profile quite peaks at around 232 ms.

4. Summary

The plasma performance of Heliotron J was improved using supersonic molecular beam injection (SMBI) as a fueling method. The time evolution of the electron density profile was measured using a microwave amplitude modulation (AM) reflectometer in the Heliotron-J SMBI plasma. Immediately after the SMBI pulse, for the case in which the SMB penetrates deeply, the density profile rapidly becomes peaked and the electron density increases in both the core and edge regions. Afterward, while the line-averaged density monotonically increases, the density profile becomes more peaked, which is consistent with the trends observed in the edge density measured by the Langmuir probe and the peaking factor of the SX profiles measured by the AXUV array. SMBI affects particle confinement and transport, thus possibly increasing the plasma stored

energy through this peaking phase. A more detailed study is required to quantitatively estimate the relationship between the peaking phase and the particle confinement and transport.

Acknowledgements

The authors are grateful to the Heliotron J team for their excellent arrangement of the experiments. This work was partly supported by NIFS/NINS under the NIFS Collaborative Research Program (NIFS04KUHL005).

- [1] L. Yao, *New Developments in Nuclear Fusion Research* (Nova Sci. Pub, 2006) pp.61–87.
- [2] T. Mizuuchi *et al.*, *Contrib. Plasma Phys.* **50**, 639 (2010).
- [3] J. Sanchez *et al.*, *Rev. Sci. Instrum.* **63**, 4654 (1992).
- [4] V. Zhuravlev, *Proc. 26th EPS Conf. on Controlled Fusion and Plasma Phys.* (Maastricht, 1999) Vol. **23J**, p857.
- [5] M. Hirsch *et al.*, *Rev. Sci. Instrum.* **67**, 1807 (1996).
- [6] T. Estrada *et al.*, *Plasma Phys. Control. Fusion* **43**, 1535 (2001).
- [7] W.W. Xiao *et al.*, *Plasma Sci. Technol.* **8**, 133 (2006).
- [8] W.W. Xiao *et al.*, *Phys. Rev. Lett.* **104**, 215001 (2010).
- [9] W.W. Xiao *et al.*, *Rev. Sci. Instrum.* **81**, 013506 (2010).
- [10] K. Mukai *et al.*, *Contrib. Plasma Phys.* **50**, 646 (2010).
- [11] T. Obiki *et al.*, *Nucl. Fusion* **41**, 833 (2001).
- [12] T. Mizuuchi *et al.*, in *Proc. 19th PSI Conference* (San Diego, 2010) P2-70. To be published in *J. Nucl. Mater.*